SLAC-PUB-12884

RECENT RESULTS ON CHARM AND TAU PHYSICS FROM *BABAR* AND BELLE

Fabrizio Salvatore
Royal Holloway, University of London
for the *BABAR* and Belle collaborations

Abstract

Recent results on charm and tau physics obtained at the *BABAR* and Belle experiments are presented in this article. The charm section will be focused on the most recent results on $D^0\overline{D}^0$ mixing at Belle and on the measurement of the pseudoscalar decay constant f_{D_s} using charm tagged e^+ e^- events at *BABAR* In the tau section, the recent results on Lepton Flavour Violation from tau decays will be discussed, as well as the recent result on the rare decay $\tau^- \to 3\pi^- 2\pi^+ 2\pi^0 \nu_\tau$ at *BABAR* and the measurement of the τ lepton mass at Belle.

Contributed to 20th Rencontres de Physique de La Vallee d'Aoste: Results and Perspective in Particle Physics,
03/05/2006--3/12/2006, La Thuile, Aosta Valley, Italy

Work supported in part by US Department of Energy contract DE-AC02-76SF00515
SLAC, Stanford University, Stanford, CA 94025

1 Introduction

B-factories have been succesfully operating for more than 6 years, providing an unprecedented data sample of $e^+e^- \to$ hadrons events. The *BABAR* and Belle experiments have in fact already collected over 330 fb^{-1} and 550 fb^{-1} respectively at the $\Upsilon(4s)$ center-of-mass energy. At this energy, the cross-section for charm and tau production is of the same order of the cross-section for b production: $\sigma(b\bar{b}) \approx 1.1\ nb \approx \sigma(c\bar{c}) \approx 1.3\ nb \approx \sigma(\tau^+\tau^-) \approx 0.9\ nb$. For this reason, B-factories can now be considered also Charm and Tau-factories.

In this paper the most recent results on both charm and tau physics from *BABAR* and Belle are presented.

2 Description of the experiments

The *BABAR* [1] detector operates at the PEPII asymmetric e^+e^- collider. Charged particles are detected and their momenta measured with a 5-layer double sided silicon vertex tracker (SVT) and a 40-layer drift chamber (DCH) inside a 1.5 T super-conducting solenoidal magnet. A quartz bar ring-imaging Čerenkov detector (DIRC) complements $\mathrm{d}E/\mathrm{d}x$ in the drift chambers for the identification of charged particles. Energies of neutral particles are measured by an electromagnetic calorimeter (EMC) composed of 6,580 CsI(Tl) crystals, and the instrumented magnetic flux return (IFR) is used to identify muons and K^0_L mesons.

The Belle [2] detector operates at the KEKB [3] asymmetric e^+e^- collider. The detector consist of a silicon vertex detector (SVD), a 50-layer central drift chamber (CDC), an array of aerogel threshold Čerenkov counters (ACC), a barrel-like arrangement of time-of-flight scintillation counters (TOF) and an electromagnetic calorimeter (ECL) comprised of CsI(Tl) crystals. All these detectors are located inside a super-conducting solenoidal coil that provides a 1.5 T magnetic field. An iron flux return outside the coil is instrumented to identify muons and K^0_L mesons (KLM).

3 Results on charm physics

3.1 Search for $D^0\overline{D}^0$ mixing in $D^0 \to K^+\pi^-$ decays

The phenomenon of quark mixing has been observed so far in the $K^0\overline{K}^0$ and $B^0\overline{B}^0$ systems, but not in the $D^0\overline{D}^0$ system. The parameters that characterize the mixing are $x \equiv \Delta m/\bar{\Gamma}$ and $y \equiv \Delta\Gamma/(2\bar{\Gamma})$, where Δm and $\Delta\Gamma$ are the differences in mass and decay width between the two mass eigenstates and $\bar{\Gamma}$ is the average width. Within the Standard Model (SM) the rate of $D^0\overline{D}^0$ mixing is expected to be small [4], where the largest values predicted are of

the order $|x| \leq |y| \sim (10^{-3} - 10^{-2})$. Observation of a much larger mixing ($|x| >> |y| \sim (10^{-3} - 10^{-2})$) or CP violation (CPV) in $D^0\overline{D}^0$ mixing would constitute unambiguous evidence for new physics.

A search for D mixing has been recently published by the Belle experiment, reconstructing the "wrong-sign" (WS) process $D^0 \to K^+\pi^-$ from a sample of 400 fb^{-1} of data [5]. This process can proceed either through directly doubly-Cabibbo-suppressed (DCS) decay or through $D^0\overline{D}^0$ mixing followed by the "right-sign" (RS) Cabibbo-favoured (CF) decay $D^0 \to \overline{D}^0 \to K^+\pi^{-1}$. The decay-time distribution of the two different decays can be employed in order to distinguish between them. Assuming negligible CPV, the decay-time distribution for $D^0 \to K^+\pi^-$ can be expressed as:

$$\frac{dN}{dt} \propto e^{-\bar{\Gamma}t}\left[R_D + \sqrt{R_D}\; y'(\bar{\Gamma}t) + \frac{x'^2 + y'^2}{4}(\bar{\Gamma}t)^2\right] , \qquad (1)$$

where R_D is the ratio of DCS to CF decay rates, $x' = x\cos\delta + y\sin\delta$, $y' = y\cos\delta - x\sin\delta$ and δ is the strong phase difference between DCS and CF amplitudes. The first (last) term in brakets is due to the DCS (CF) amplitude, while the middle one is due to the interference between the two amplitudes. The time integrated rate (R_{WS}) for $D^0 \to \overline{D}^0 \to K^+\pi^-$ relative to that of $D^0 \to \overline{D}^0 \to K^-\pi^+$ is given by $R_D + \sqrt{R_D}\; y' + (x'^2 + y'^2)/2$.

In order to allow for CPV, Eq. 1 is applied separately to D^0 and $\overline{D}^0$, resulting in six observables: R_D^+, x'^{+2}, y'^+ for D^0 and R_D^-, x'^{-2}, y'^- for $\overline{D}^0$. CPV is parametrized by the asymmetries $A_D = (R_D^+ - R_D^-)/(R_D^+ + R_D^-)$ and $A_M = (R_M^+ - R_M^-)/(R_M^+ + R_M^-)$, where $R_M^\pm = (x'^\pm + y'^\pm)/2$. A_D and A_M characterize CPV in DCS decays and mixing respectively.

The detailes of the selection criteria for this analysis are reported in [5]. Signal events that satisfy the requirement $1.81 < m_{K\pi} < 1.91$ GeV/c^2 and $0 < Q < 20$ MeV are selected, where Q is the kinetic energy released in the decay. The RS and WS event yields are obtained from a two-dimensional fit to the $(m_{K\pi}, Q)$ distribution. Figure 1 shows the $m_{K\pi}$ and Q distributions superimposed with a projection of the fit result for WS events.
The four significant sources of background in the WS sample are: 1) random π background, in which a random π^+ is combined with a $\overline{D}^0 \to K^+\pi^-$ decay; 2) $D^{*+} \to D^0\pi^+$ events, followed by D^0 decaying to $\geq$ 3-body final states; 3) $D^+_{(s)}$ decays and 4) combinatorial background. These background shapes are obtained from Monte Carlo (MC) and fixed in the fit. The result of the fit is 1073993 ± 1108 RS and 4024 ± 88 WS events, corresponding to $R_{WS} = (0.375 \pm 0.008)\%$ (statistical error only).

[1] Charged-conjugate modes will always be implied throughout this paper, unless otherwise noted.

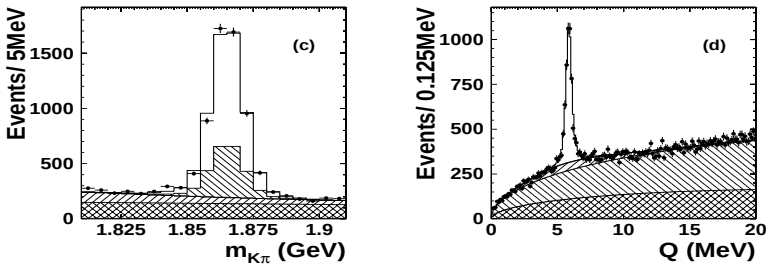


Figure 1: *D mixing analysis: distribution of (c) WS* $m_{K\pi}$ *with* $5.3 < Q < 6.5$ *MeV and (d) WS* Q *with* $1.845 < m_{K\pi} < 1.885$ *GeV/*c^2*. Superimposed on the data (points with error bars) are projections of the* $(m_{K\pi}, Q)$ *fit.*

The mixing parameters R_D, x'^2, y' of Eq. 1 are obtained using an unbinned maximum likelihood fit to the distribution of the WS proper decay-time, considering the 4σ region $|m_{K\pi} - m_{D^0}| < 22$ MeV/c^2 and $|Q - 5.9\,\mathrm{MeV}| < 1.5$ MeV. The likelihood function is constructed from the probability density functions (PDF) for signal and backgrounds, where each pdf depends on the decay-time, the invariant mass $m_{K\pi}$, the kinetic energy Q and the expected error on decay time, estimated from the covariance matrix of the vertex fit. The results of the fits to the WS proper decay-time are summarized in Table 1. In The first fit, CP is assumed to be conserved and the projection of this fit superimposed on the data is shown in Figure 2. The χ^2 of the projection in 54.6 for 60 bins. The central value of x'^2 is in the physically-allowed region $x'^2 > 0$. Figure 2 shows the 95% CL contours with and without CPV allowed that are obtained using the Feldman-Cousins method [6]. In the case of no CPV, the no-mixing point $x'^2 = y' = 0$ lies just outside the 95% CL contour and corresponds to 3.9% CL (systematic uncertainty included).

3.2 Precise measurement of the presudoscalar decay constant f_{D_s} using charm tagged e^+ e^- events

The measurement of leptonic weak decays of charmed pseudoscalar mesons can provide a determination of the overlap between the wavefunction of heavy and light quarks within the meson, represented by the a form factor f_M for each meson M. The partial width for a D_s^+ meson to decay weakly to a lepton l is given by:

$$\Gamma(D_s^+) = \frac{G_F^2 |V_{cs}|^2}{8\pi} f_{D_s}^2 m_l^2 m_{D_s} \left(1 - \frac{m_l^2}{m_{D_s}^2}\right)^2 , \qquad (2)$$

Table 1: *Summary of the fit result in the D mixing analysis obtained from the separate likelihood fits. The 95% CL intervals are obtained using the Feldman-Cousins method.*

Fit Case	Parameter	Fit Result ($\times 10^{-3}$)	95% CL ($\times 10^{-3}$)
no CPV	R_D	3.64 ± 0.17	$(3.3, 4.0)$
	x'^2	$0.18^{+0.21}_{-0.23}$	< 0.72
	y'	$0.6^{+4.0}_{-3.9}$	$(-9.9, 6.8)$
	R_M	-	$(0.63 \times 10^{-}5, 0.40)$
CPV	A_D	23 ± 47	$(-76, 107)$
	A_M	670 ± 1200	$(-995, 1000)$
	x'^2	-	< 0.72
	y'	-	$(-28, 21)$
	R_M	-	$< 0.40)$
no mixing	R_D	$3.77 \pm 0.08 \pm 0.05$	

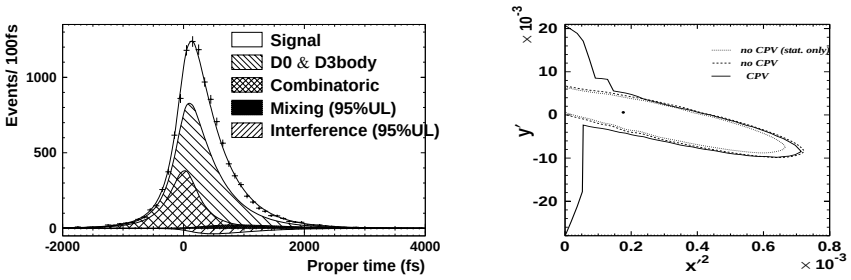


Figure 2: *D mixing analysis: (left) decay-time distribution for WS events satisfying* $|m_{K\pi} - m_{D^0}| < 22\ MeV/c^2$ *and* $|Q - 5.9\ MeV| < 1.5\ MeV$*. Superimposed on the data (points with error bars) are projections of the decay-time fit when no CPV is assumed. (right) 95% CL regions for* (x'^2, y')*.*

where m_l and m_{D_s} are the lepton and D_s masses, G_F is the Fermi constrant and $|V_{cs}|$ is the CKM parameter for the annihilation of the quarks in the D_s. Predictions from lattice QCD have yielded $f_{D_s} = (249 \pm 17)$ MeV and $f_{D_s}/f_D = 1.24 \pm 0.07$ [7], while CLEO-c has recently measured $f_D = (223 \pm 17)$ MeV [8].

BABAR has presented at this conference a preliminary result of the measurement of the ratio $\Gamma(D_s^+ \to \mu^+\nu_\mu)/\Gamma(D_s^+ \to \phi\pi^+)$ and of the decay constant f_{D_s} using a sample of 230 fb^{-1} of data [10]. The $D_s^+ \to \mu^+\nu_\mu$ events are reconstructed from the decay chain $D_s^{*+} \to \gamma D_s^+$, $D_s^+ \to \mu^+\nu_\mu$, where the D_s^{*+} are produced in the hard fragmentation of continuum $c\bar{c}$ events. In the D_s^{*+} decay an energetic photon, a high-momentum D_s^+ and a daughter muon and neutrino are produced, all lying mostly in the same hemisphere of the event. The recoil system of a signal candidate is a fully reconstructed D^0, D^+, D_s^+ or D^{*+} (referred to as the "tag" system), wherein the tag flavour, and so the charge of the signal muon, is uniquely determined. A minimum tag momentum close to the kinematic limit for charm mesons produced in B decays is required in order to reduce B backgrounds. The D_s^{*+} signal is reconstructed from a muon and photon candidate in the recoil of the tag. Muons are identified using the IFR and must have a momentum greater than 1.2 GeV/c in the center-of-mass frame (CM) and a charge consistent with the tag flavour. Energy deposits in the EMC with no associated charged track are identified as photon candidates, and the candidates CM energy must be greater than 0.115 GeV. The total missing energy and momentum in the CM (E^*_{miss}, p^*_{miss}) is computed using the four-momenta of the incoming e^+e^- and the measured four-momenta of all tracks and photons in the event. To take into account that the neutrino in the signal decay leads to a large missing energy in the event, signal candidates are selected requesting $E^*_{miss} > 0.38$ GeV. The CM four-momentum of the D_s^+ candidate $(\vec{p}^*_{D_s^+})$ is obtained combining the CM four-momenta of the neutrino (estimated using a technique adopted from [9]) and the muon. The D_s^+ candidate is then combined with a photon candidate to form the D_s^{*+}. Signal events are required to have $|\vec{p}^*_{D_s^{*+}}| > 3.55$ GeV/c. The signature of the $D_s^{*+} \to \gamma D_s^+$ decay is a narrow peak in the distribution of the mass difference $\Delta M = M(\mu\nu\gamma) - M(\mu\nu)$ at 143.5 MeV/c^2.

There are several distinct sources of background that have been taken into account in the analysis. The first type of backgrounds are $e^+e^- \to f\bar{f}$ events ($f = u, d, s, b$ or τ) without a real charm tag or $e^+e^- \to c\bar{c}$ events where the tag is incorrectly reconstructed. The contribution of these events is estimated from real data using the tag side-bands. The second type of background events are correctly tagged $c\bar{c}$ events with the selected muon coming from a semileptonic charm decay or $\tau^+ \to \mu^+\nu_\mu\bar{\nu}_\tau$. The size and shape of this contribution is estimated by repeating the analysis substituting a well-identified electron for the muon. The ratio of muon to electron efficiency is applied as a weight to

each electron event. The remaining backgrounds are estimated using Monte Carlo simulations.

Data events selected in the analysis are grouped in four sets, according on whether the tag is in the signal or side-band region and on whether the selected lepton is a muon or an electron. The ΔM distribtion for events in the tag side-bands is subtracted from the signal distribution and finally the electron distribution is subtracted from the muon one. The resulting ΔM distribution (Figure 3) is then fitted with the function $(N_{sig} f_{sig} + N_{bg} f_{bg})(\Delta M)$, where f_{sig} and f_{bg} describe the simulated signal and background ΔM distribution. All parameters in the fit are fixed, except N_{sig} and N_{bg} and the result of the fit yields $N_{sig} = 489 \pm 55$(stat) events.

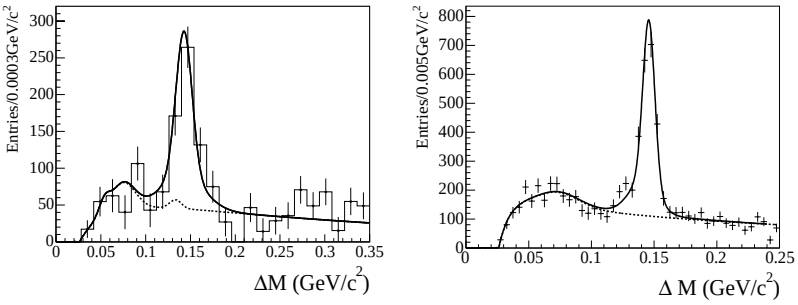


Figure 3: *f_{D_s} analysis: (left) ΔM distribution for $D_s^+ \to \mu^+ \nu_\mu$ events after the tag side-bands and the electron sample are subtracted. The solid line is the fitted signal + background distribution, while the dotted line is the background distribtion alone. (right) ΔM distribution for $D_s^+ \to \phi \pi^+$ events after the tag side-bands are subtracted. The solid line is the fitted signal + background distribution, while the dotted line is the background distribtion alone.*

Since the $D_s^{(*)+}$ production rate in $c\bar{c}$ is unknown, the partial width ratio $\Gamma(D_s^+ \to \mu^+ \nu_\mu)/\Gamma(D_s^+ \to \phi \pi^+)$ is computed by reconstructing the decay chain $D_s^{*+} \to \gamma D_s^+$, $D_s^+ \to \phi \pi^+$ and the $D_s^+ \to \mu^+ \nu_\mu$ branching fraction is computed using the known branching fraction for $D_s^+ \to \phi \pi^+$.

Candidate ϕ mesons are reconstructed from two kaons of opposite sign and then combined with a charged pion to form a D_s^+ candidate. Photon candidates are then combined with the reconstructed D_s^+ to form D_s^{*+} candidates. The same requirements on the photon CM energy and D_s^{*+} momentum as in the $D_s^+ \to \mu^+ \nu_\mu$ selection are applied. The data events are then grouped in two sets, according on whether the tag is in the signal or side-band region, and after the tag side-band Δm distribution has been subtracted from the tag signal one, the resulting distribution is fitted with the function $(N_{\phi\pi} f_{\phi\pi} + N_{\phi\pi bg} f_{\phi\phi bg})(\Delta M)$. The fit yields $N_{\phi\pi} = 2065 \pm 95$(stat) events (Figure 3).

The presence of two charged kaons in the $D_s^+ \to \phi\pi^+$ events leads to an increase in the number of random tag combinations with respect to $D_s^+ \to \mu^+\nu_\mu$ events. The correction for this effect is determined from MC and is found to be 1.4%. The effect of a difference between data and MC in the D_s^{*+} spectrum is measured by selecting $D_s^{*+} \to \gamma D_s^+$, $D_s^+ \to \phi\pi^+$ events in data and removing the requirement on $|\vec{p}^*_{D_s^{*+}}|$. A harder momentum spectrum is observed in data when efficiency corrected D_s^{*+} events are compared with those selected from MC. Therefore, the detection efficiencies for signal $D_s^{*+} \to \gamma D_s^+$, $D_s^+ \to \phi\pi^+$ events are re-evaluated after weighting the simulated events to match the D_s^{*+} momentum spectrum in data. Once these efficiency corrections are applied, the partial width ratio is determined to be $\Gamma(D_s^+ \to \mu^+\nu_\mu)/\Gamma(D_s^+ \to \phi\pi^+) = 0.136 \pm 0.017(\text{stat})$, with $\mathcal{B}(\phi \to K^+K^-) = 49.1\%$ [11].

The total systematic uncertainty in $\Gamma(D_s^+ \to \mu^+\nu_\mu)/\Gamma(D_s^+ \to \phi\pi^+)$ is 4.6% and is dominated by the systematic error in the signal efficiency and the uncertainty arising from a possible inadequate parametrization of the signal and background shapes.

Using the *BABAR* measurement $\mathcal{B}(D_s^+ \to \phi\pi^+) = (4.81 \pm 0.64)\%$ [12], the branching fraction $\mathcal{B}(D_s^+ \to \mu^+\nu_\mu) = (6.5 \pm 0.8 \pm 0.3 \pm 0.9) \times 10^{-3}$ and the decay constant $f_{D_s} = (279 \pm 17 \pm 6 \pm 19)$ MeV are obtained. The third error in the measurement is due to the uncertainty in the $D_s^+ \to \phi\pi^+$ branching fraction. The ratio of f_{D_S} to f_D from the CLEO-c measurement is $f_{D_s}/f_D = 1.25 \pm 0.14$ and is consistent with the lattice QCD prediction.

4 Results on tau physics

4.1 Search for Lepton Flavour Violation in tau production and decay

The fermion mass matrices and the mechanism of electroweak symmetry breaking are not explained within the minimal SM. In the SM, lepton-flavour violation (LFV) is not a conserved quantity and evidence for neutrino oscillation indicate a violation of the lepton-flavour symmetry in the neutral sector [13].

The most stringent limits on branchig ratios of neutrinoless decays are for rare muon decays and are of the order of 10^{-12} [14, 15]. Many theoretical models with mass-dependent couplings give an enhancement of the branching fraction for τ decays over the corresponding μ decays [16, 17, 18], justifying the effort of looking for LFV in τ decays.

A summary of the limits on LFV in τ decays obtained by *BABAR* [19] and Belle [20] is given in Table 2. These represent the most stringent limits so far on LFV in such decay channels.

A recent Belle analysis on the search for LFV in τ^- decays with a K_s^0 meson on 281 fb^{-1} of data has been presented at this conference and will be

Table 2: *Summary of the LFV results from the BABAR and Belle Collaborations.*

LFV decay mode	*BABAR* upper limit	Belle upper limit
$\tau \to e\gamma$	1.10×10^{-7}	3.90×10^{-7}
$\tau \to \mu\gamma$	0.68×10^{-7}	3.10×10^{-7}
$\tau \to lll$	$(1.1 - 3.3) \times 10^{-7}$	$(1.9 - 3.5) \times 10^{-7}$
$\tau \to lhh'$	$(0.7 - 4.8) \times 10^{-7}$	$(1.6 - 8.0) \times 10^{-7}$
$\tau \to l(\pi^0, \eta, \eta')$	-	3.90×10^{-7}
$\tau \to lV^0$	-	$(2.0 - 7.7) \times 10^{-7}$
$\tau \to \lambda\pi, \lambda\pi$	-	$(1.40,\ 0.72) \times 10^{-7}$

described in the following.

4.1.1 Search for LFV τ^- decays with a K_s^0 meson

A detailed description of the selection criteria for this analysis can be found in [21]. $\tau^+\tau^-$ events are selected with one τ (signal side) decaying into a charged lepton (either e or μ) and a K_s^0, decaying into $\pi^+\pi^-$, and the other τ (tag side) decaying into one charged particle (of opposide sign to the lepton) with any number of additional photons. Particle identification is essential in this analysis and it is obtained using likelihood variables based on the information of the appropriate subdetectors.

Signal events are isolated by requiring that the total net charge of the four charges in the event is zero and that the magniture of the thrust of the event is greater than 0.9, to suppress $q\bar{q}$ background. The event must have a 3-1 topology configuration relative to the plane perpendicular to the thrust axis. The K_s^0 is reconstructed from two opposite charged pions with an invariant mass within $0.482\ \mathrm{GeV/c^2} < M_{\pi^+\pi^-} < 0.514\ \mathrm{GeV/c^2}$ and with a vertex that is displaced from the interaction point in the direction of the pion pair momentum. Lepton identification is applied to each track, except those forming the K_s^0 candidate on the signal side. To ensure that the missing momentum in the event is only due to the non indentified neutrinos, the magnitude of $\vec{p}_{miss}$ is required to be greater than 0.4 GeV/c and its direction is required to point into the fiducial volume of the detector. Since the neutrinos are emitted only in the tag side, the direction of $\vec{p}_{miss}$ should lie in the tag side of the event. Background coming from generic $\tau^+\tau^-$ events and continuum is removed looking at the correlation between the reconstructed momentum of the lK_s^0 system and the cosine of the opening angle between the lepton and the K_s^0. The final efficiencies for the $\tau^- \to e^- K_S^0$ and $\tau^- \to \mu^- K_S^0$ decay modes are 15.0% and 16.2%

respectively.

Signal candidates are selected looking at the two-dimensional plot of the lK_s^0 invariant mass M_{inv} and the difference of their energy from the beam energy in the CM system, ΔE. For the signal events, M_{inv} should be close to the τ mass and ΔE should be close to zero. The resolutions of M_{inv} and ΔE are parametrized from the MC distributions around the peak, with bifurcated Gaussian shapes to take into account for initial state radiation. Figure 4 shows the $(M_{inv}, \Delta E)$ plot for data and signal MC samples distributed over $\pm 15\sigma$ in ΔE and M_{inv}.

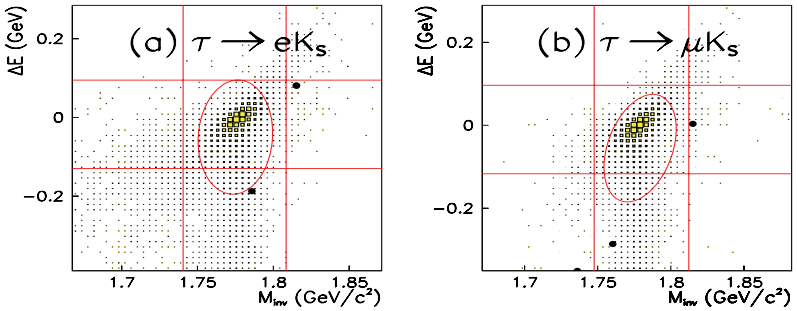


Figure 4: *LFV $\tau^- \to l^- K_s^0$ analysis: scatter plot of the data and signal MC events in the $(M_{inv}, \Delta E)$ plane for the (a) $\tau^- \to e^- K_S^0$ and (b) $\tau^- \to \mu^- K_S^0$ analysis. The eliptical signal region shown by a solid curve is used to evaluate the signal yield.*

In order not to bias the criteria to select the signal events, a region of $\pm 5\sigma$ in M_{inv} and of -0.5 GeV $< \Delta E < 0.5$ GeV in data is blinded. To optimize the sensitivity of the analysis, the signl yield is obtained by selecting the events using an elliptically shaped signal region, which has major and minor axes that correspond to $\pm 5\sigma$ in the MC resolution for the $(M_{inv}, \Delta E)$ plane. The signal efficiencies for this region after all requirements are 11.8% for the $\tau^- \to e^- K_S^0$ mode and 13.5% for the $\tau^- \to \mu^- K_S^0$ one. The remaining background events in the signal ellipse are evaluated using the M_{inv} side-band regions, extrapolating into the signal region under the assumption that the background distribution is flat in M_{inv}. The expected background obtained is 0.2 ± 0.2 events for each mode.

No statistically significant excess of data events is observed after unblinding the signal region, therefore a frequentist approach is used to compute the upper limits for the signal yields [6]. At 90% CL, the resulting limits are $s_{90} = 2.23$ events in both modes and the obtained upper limits on the branching fraction (before including the systematic errors) are computed as

$$\mathcal{B}(\tau^- \to l^- K_s^0) = \frac{s_{90}}{2\epsilon N_{\tau\tau}\mathcal{B}(K_s^0 \to \pi^+\pi^-)} \ , \qquad (3)$$

where $N_{\tau\tau} = 250 \times 10^6$ is the total number of $\tau\tau$ pairs and $\mathcal{B}(K_s^0 \to \pi^+\pi^-) = 0.6895\%$ [11]. The obtained values are $\mathcal{B}(\tau^- \to e^- K_S^0) < 5.5 \times 10^{-8}$ and $\mathcal{B}(\tau^- \to \mu^- K_S^0) < 4.8 \times 10^{-8}$. The total systematic uncertainty is 6.5% and is dominated by the K_s^0 detection efficiency and the tracking efficiency. The upper limits on the branchin fractions at 90% CL including these systematic uncertainties are computed using the POLE program without conditioning [22]. The resulting values are:

$$\begin{aligned} \mathcal{B}(\tau^- \to e^- K_s^0) &< 5.6 \times 10^{-8} \\ \mathcal{B}(\tau^- \to \mu^- K_s^0) &< 4.9 \times 10^{-8} \ . \end{aligned}$$

4.1.2 Search for $e^+e^- \to \mu^+\tau^-$ and $e^+e^- \to e^+\tau^-$ reactions

Tests for LFV in the τ production process $e^+e^- \to l^+\tau^-$, where l^+ is an electron or a muon, have been performed at a number of CM energies ($\sqrt{s}$), but have so far given far less stringent limits on LFV than the test made on τ decays. These limits are summarized in Table 3.

Table 3: *Summary of the experimental limits on the LFV process $e^+e^- \to l^+\tau^-$.*

	$\sqrt{s}$ (GeV)	UL (95% CL)	Publication
$\sigma_{\mu\tau}/\sigma_{\mu\mu}$	29	$< 6.1 \times 10^{-3}$	Phys. Rev. Lett. **66**, 1007 (1991)
$\sigma_{e\tau}/\sigma_{\mu\mu}$	29	$< 1.3 \times 10^{-3}$	Phys. Rev. Lett. **66**, 1007 (1991)
$\mathcal{B}(Z^0 \to \mu\tau, e\tau)$	92	$< (0)1 \times 10^{-3}$	Phys. Lett. **254**, 293 (1991)
$\sigma_{\mu\tau}$	> 92	64 fb	Phys. Lett. **519**, 23 (2001)
$\sigma_{e\tau}$	> 92	78 fb	Phys. Lett. **519**, 23 (2001)

A preliminary measurement from the *BABAR* experiment has been presented at this conference on the search for the $e^+e^- \to l^+\tau^-$ process at the lower energies accessible by the B-factory detectors. The results presented are referred to four modes of the above process, where l^+ is an electron or a muon and the τ^- decays to either $\pi^-\pi^+\pi^-\nu_\tau$ or $\pi^-\nu_\tau$. The data sample corresponds to an integrated luminosity of 210.6 fb^{-1} recorded at the CM energy of $\sqrt{s} = 10.58$ GeV.

Signal and background events are simulated in order to evaluate the selection efficiencies, background contamination and for studing systematic effects in the analysis. However, the final background estimation relies solely on the data. The generator used for the τ-pair events is the `KK2f` MC generator [23];

τ decays are then modeled with TAUOLA [24] according to measured rates. The $\tau^- \to \pi^-\pi^+\pi^-\nu_\tau$ decay is simulated assuming an intermediate $a_1^-(980)$ axial-vector state [11, 25]. Continuum background events, as well as di-muon, Bhabha, $B\bar{B}$ and two-photon events are also generated [26]. The response of the detector is simulated using GEANT [27].

The signature of the signal process in the CM frame is the presence of an isolated high-momentum muon or electron recoiling against one or three charged track in the tag-side of the event. The invariant mass of the recoling pions plus the missing neutrino should be consistent with the τ mass [11].

All charged tracks are required to be within the acceptance of the EMC, DIRC and IFR, that are used for particle identification. The events are selected requiring that one of the tracks is a well identified muon or electron with CM momentum greater than 4.68 GeV/c, and no other track satisfy the lepton or kaon identification criteria. Two hemispheres are defined with respect to the plane perpendicular to the thrust axis of the event, computed using all identified charged and neutral tracks. The identified lepton is required to be in one of the two hemispheres, while all remaining tracks are required to be in the opposite one. The momentum of the candidate τ^- is defined as $|p^*_\tau| = \sqrt{E^{*2}_\tau - m^2_{\tau PDG}}$, where $E_\tau = (\sqrt{s}/2 + (m^2_{\tau PDG} - m^2_{lPDG})/2\sqrt{s})$. Its direction is assumed to be the opposite of the e^+/μ^+ candidates. The reconstructed τ mass is defined to be $m_\tau = \sqrt{(E^*_\pi + p^*_\nu)^2 - |p^*_\tau|^2}$, where E^*_π is the CM energy of the pions and the momentum of the missing neutrino is $p^*_\nu = p^*_\tau - p^*_\pi$. Signal events are retained if the difference between the e^+/μ^+ candidate CM energy and $\sqrt{s}/2$ satisfy the condition -0.5 GeV $\leq \Delta E \leq 0.2$ GeV. True signal events are expected to have $\Delta E \sim -0.15$ GeV, while generic $\tau^+\tau^-$ events will peak at zero and other backgounds will have a large negative ΔE.

Other kinematic variables are employed to further suppress the backgrounds. The missing energy in the CM system E^*_{miss} will peak at zero or near $\sqrt{s}/2$ for many backgrounds, while it is uniformly distributed in signal events. Also, the reconstructed missing mass squared m^2_{miss} should be consistent with zero. Events with photons or neutral pions are removed with a requirement on neutral energy cluster in the detector. Events where particles are lost within the beam pipe are removed requiring that the cosine of the angle between the direction of the neutrino and the beam axis in the CM system is within the detector acceptance. Finally, events with back-to-back tracks are rejected using the cosine of the angle between the direction of the neutrino and the τ.

The signal yield is extracted using a maximum likelihood fit to the m_τ and p^*_l variables only for those selected events that fall in the two-dimensional region defined by 1.6 GeV/c^2 $< m_\tau <$ 2.0 GeV/c^2 and 4.9 GeV/c $< p^*_l <$ 5.32 GeV/c (5.02 GeV/c $< p^*_l <$ 5.32 GeV/c for the $\tau^- \to \pi^-\nu_\tau$ events). The main background comes from generic $\tau^+\tau^-$ events, where the τ^+ decays to e^+/μ^+

plus a neutrino and the τ^- decays in either $\pi^-\pi^+\pi^-\nu_\tau$ or $\pi^-\nu_\tau$. Background from light quark continuum contributes significantly only to the $e^+e^- \to \mu^+\tau^-$ ($\tau^- \to \pi^-\pi^+\pi^-\nu_\tau$) process, while $e^+e^- \to \mu^+\mu^-$ events only contribute to the $e^+e^- \to \mu^+\tau^-$ ($\tau^- \to \pi^-\nu_\tau$) process. All other backgrounds are negligible. The likelihood for the selacted sample is given by the product of the PDF $\mathcal{P}_j = \mathcal{P}_j(m_\tau)\mathcal{P}_j(p_l^*)$ for each event candidate i:

$$\mathcal{L} = \frac{e^{-\sum_j n_j}}{N!} \prod_i^N \sum_j n_j \mathcal{P}_j^i \ , \tag{4}$$

where n_j is the yield of events for the hypothesis j found in the fit and N is the total number of events in the sample. The PDF for signal events is obtained using double Crystal Ball functions [28] for both m_τ and p_l^*, while for non signal events a two-dimensional non-parametric PDF obtained from MC events is used [29].

The largest contribution to the systematic error of the analysis comes from the variation of the PDF fit parameters and from the expected resolution of the selected variables. Also, a contribution to the systematic error coming from the modeling of the $\tau^- \to \pi^-\pi^+\pi^-\nu_\tau$ decay in the MC is taken into account. The results of the analysis are summarized in Table 4.

Table 4: *Summary of the results of the $e^+e^- \to l^+\tau^-$ analysis. The first error is statistical and the second is systematic.*

$e^+e^- \to \mu^+\tau^-$	$\tau^- \to \pi^-\pi^+\pi^-\nu_\tau$	$\tau^- \to \pi^-\nu_\tau$
Signal events	$-1.37 \pm 9.9 \pm 2.6$	$-1.37 \pm 9.9 \pm 2.6$
$\sigma_{\mu\tau}$ (fb)	$-0.35 \pm 2.6 \pm 0.7$	$0.85 \pm 4.5 \pm 2.0$
$\sigma_{\mu\tau}$ (95% CL)	$< 5.91\ fb$	$< 11.4\ fb$
$\sigma_{\mu\tau/\mu\mu}$ (95% CL)	$< 5.2 \times 10^{-6}$	$< 10.1 \times 10^{-6}$

$e^+e^- \to e^+\tau^-$	$\tau^- \to \pi^-\pi^+\pi^-\nu_\tau$	$\tau^- \to \pi^-\nu_\tau$
Signal events	$15.9 \pm 10.3 \pm 2.7$	$10.7 \pm 8.8 \pm 2.7$
$\sigma_{e\tau}$ (fb)	$6.5 \pm 4.2 \pm 1.1$	$3.9 \pm 3.2 \pm 1.0$
$\sigma_{e\tau}$ (95% CL)	$< 14.8\ fb$	$< 11.1\ fb$
$\sigma_{e\tau/\mu\mu}$ (95% CL)	$< 13.1 \times 10^{-6}$	$< 9.8 \times 10^{-6}$

Combining the results obtained for the $\tau^- \to \pi^-\pi^+\pi^-\nu_\tau$ and $\tau^- \to \pi^-\nu_\tau$ decays, the 95% CL upper limits on the cross-sections for $e^+e^- \to \mu^+\tau^-$ and $e^+e^- \to e^+\tau^-$ reactions are calculated: $\sigma_{\mu\tau} < 4.6\ fb$, $\sigma_{e\tau} < 10.1\ fb$. The 95% CL upper limits on the ratio of the cross-sections with respect to the

$e^+e^- \rightarrow \mu^+\mu^-$ cross-section are calculate to be $\sigma_{\mu\tau/\mu\mu} < 4.0 \times 10^{-6}$ and $\sigma_{e\tau/\mu\mu} < 8.9 \times 10^{-6}$.

4.2 Search for the decay $\tau^- \rightarrow 3\pi^- 2\pi^+ 2\pi^0 \nu_\tau$

Hadronic decays of the τ lepton provide an excellent laboratory for the study of strong interactions. Decays of the τ in one or three charged tracks have been well studied in the past. High multiplicity τ decay (5 or 7 prongs) have much lower branching ratios but the unprecedented integrated luminosity reached by the B-factory experiment now allows detailed searches for these high multiplicity τ decay modes.

The *BABAR* experiment has recently published an analysis on the search for the $\tau^- \rightarrow 3\pi^- 2\pi^+ 2\pi^0 \nu_\tau$ decay [30] in 232 fb^{-1} of data. This mode is highly suppressed because of the limited phase space for the decay of the τ into seven particles [31, 32]. For this reason, it is of particular interest because, if observed, it may lead to a more stringent limit on the τ neutrino mass.

Events with six charged tracks coming from the interaction point and minimum transverse momenta of 100 MeV/c are selected. Photons are reconstructed from clusters in the EMC with a minimum deposit of 50 MeV and a lateral energy profile consistent with that of a photon. Neutral pions are reconstructed from photon candidates, requiring their invariant mass to be within 113 and 155 MeV/c^2 (120 and 148 Mev/c^2 of π^0 candidates with 300 MeV $< E_{\pi^0} <$ 450 MeV). Only π^0 candidates with $E_{\pi^0} > 300$ MeV are retained. Since τ-pair events are produced approximately back-to-back in the CM system, the event can be divided in two hemispheres by the plane perpendicular to the thrust axis. One hemisphere is required to have only one charged track (tag-side), while the other hemisphere contains the remaining 5 charged tracks (signal-side). Only events where there are exactly 2 candidate π^0s in the signal-side are retained.

To reduce $B\bar{B}$ and continuum background, the magnitude of the thrust is required to be greater than 0.9. To further reduce the continuum background, the track in the tag-side of the event has to be identified as an electron or a muon, with at most one additional photon in the tag-side with $E_\gamma < 500$ MeV. Four out of five charged tracks in the signal-side are required to be identified as pions with high probability, while a looser identification is applied to the fifth track. This requirement reduces particularly the background from generic τ events with one converted photon and $e^+e^- \rightarrow q\bar{q}$ containing kaons. The total visible energy in the CM, obtained as the sum of the CM energy of all charged tracks and reconstructed π^0s, is required to be less than the beam energy $E_{beam} = 5.29$ GeV. To suppress background from $e^+e^- \rightarrow q\bar{q}$, the residual energy E_{res}, defined as the neutral energy on the signal-side not associated to the reconstructed τ decay products, is required to be less than 300 MeV.

The signal yield is computed in the signal region defined by $1.3\,\mathrm{GeV/c^2} < M_\tau^* < 1.8\,\mathrm{GeV}/c^2$, where M_τ^* is the pseudo-mass of the τ [33]. The pseudo-mass is defined by: $M_\tau^{*2} = 2(E_{beam} - E_{7\pi})(E_{7\pi} - p_{7\pi}) + M_{7\pi}^2$, where the direction of the τ neutrino is approximated by the combined momentum vector of the seven pions and its energy by the difference between E_{beam} and $E_{7\pi}$. The advantage of M_τ^* over the invariant mass $M_{7\pi\nu}$ ia a considerably better separation of the signal from the hadronic $q\bar{q}$ background.

The signal efficiency after all cuts is computed using MC events and is found to be $(0.66 \pm 0.05)\%$. The error is a combination of statistical and systematic uncertainties, where the main systematic uncertainties come from the reconstruction of charged tracks and photons and the π^0 identification. The expected background contribution from generic τ decays is computed from MC events and it is found to be 4.3 ± 1.0. The $q\bar{q}$ background is estimated directly from the data, by subtracting the expected τ background contribution from the pseudo-mass distribution and fitting the resulting histogram in the range $1.8\,\mathrm{GeV/c^2} < M_\tau^* < 3.3\,\mathrm{GeV}/c^2$. The fit function is then extrapolated below $1.8\,\mathrm{GeV/c^2}$ and its integral between 1.3 and $1.8\,\mathrm{GeV}/c^2$ yields the $q\bar{q}$ estimate. Combining the background estimates from τ and $q\bar{q}$ events, a total of $6.5^{+2.0}_{-1.4}$ background events are expected. In the data signal region, a total of 10 events are observed, giving therefore no evidence for the $\tau^- \to 3\pi^- 2\pi^+ 2\pi^0 \nu_\tau$ decay. Figure 5 shows the final pseudo-mass spectrum in data, with superimposed the expected background PDF.

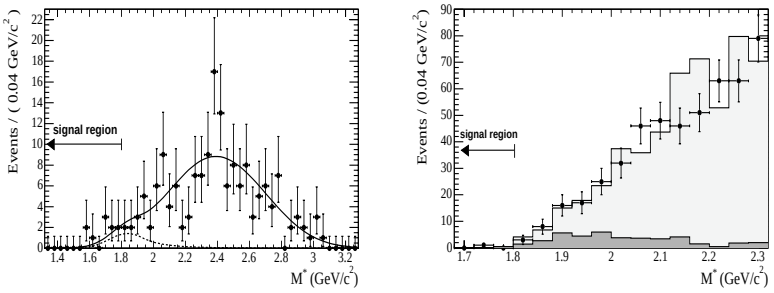


Figure 5: *$\tau^- \to 3\pi^- 2\pi^+ 2\pi^0 \nu_\tau$ analysis: (left) pseudo-mass distribution of the data events passing the $\tau^- \to 3\pi^- 2\pi^+ 2\pi^0 \nu_\tau$ selection criteria. The solid curve represents the total expected background PDF and the dashed line represents the τ background contribution. (right) pseudo-mass distribution of the data (points) and MC (histogram) events passing the $\tau^- \to 2\omega\pi^- \nu_\tau$ selection criteria. The shaded area represents the τ background contribution.*

The upper limit for the branching fraction of the $\tau^- \to 3\pi^- 2\pi^+ 2\pi^0 \nu_\tau$ decay is computed using the formula:

$$\mathcal{B}(\tau^- \to 3\pi^- 2\pi^+ 2\pi^0 \nu_\tau) = \frac{\lambda_{sig}}{2\epsilon N_{\tau\tau}} \ , \qquad (5)$$

where λ_{sig} is the upper limit on the number of signal events at the 90% CL, ϵ is the signal efficiency and $N_{\tau\tau} = 206.5 \times 10^6$ is the total number of τ-pair events. λ_{sig} is obtained using a limit calculator program [34] that follows the Cousings and Highland method [35] of incorporating systematic errors in upper limits and is found to be $\lambda_{sig} = 9.2$ events. Using this number, the upper limit on the branching fraction is $\mathcal{B}(\tau^- \to 3\pi^- 2\pi^+ 2\pi^0 \nu_\tau) < 3.4 \times 10^{-6}$, at 90% CL.

In addition to the inclusive result, also the resonant decay mode $\tau^- \to 2\omega\pi^-\nu_\tau$, with $\omega \to \pi^+\pi^-\pi^0$ is searched for. Due to its kinematics, this channel has a much narrower allowed pseudo-mass range, 1.7 GeV/c^2 $< M_\tau^* <$ 1.8 GeV/c^2. For the same reason, backgrounds are expected to be smaller.

The same event selection is applied, with the additional requirement that the ω resonance should be reconstructed as a $\pi^+\pi^-\pi^0$ combination with 0.76 GeV/c^2 $< M_{\pi^+\pi^-\pi^0} <$ 0.8 GeV/c^2. Since the reconstruction of the two ω mesons suppresses the backgrounds, the selection requirements can be substantially loosened to increase the selection efficiency. In particular, no paticle identification is applied on the tag-side, and only a loose pion identification is applied on the signal-side. As a result, the total signal efficiency is $(1.53 \pm 0.13)\%$. The background estimation is done using MC simulations and no $q\bar{q}$ contribution is expected in the signal region. The total number of expected background events is $0.4^{+1.0}_{-0.4}$. One event survives all the analysis criteria in 232 fb^{-1} of data, which is consistent with the background predictions. The pseudo-mass spectrum in data is shown in Figure 5. Using the same techniques employed in the previous measurement, the upper limit on the number of signal events at the 90% CL is $\lambda_{\omega sig} = 3.4$ events and the upper limit for the branching fraction of the decay is $\mathcal{B}(\tau^- \to 2\omega\pi^-\nu_\tau) < 5.4 \times 10^{-7}$ at 90% CL.

4.3 Measurement of the mass of the τ lepton

Masses of quarks and leptons are fundamental parameters of the SM. In particular, high precision measurements of the mass, lifetime and leptonic branching fractions of the τ lepton can be used to test lepton universality. The present PDG value of the τ mass [11] is dominated by the result of the BES Collaboration [36] and has an accuracy of about 0.3 MeV. The analysis of individual τ lepton decays allows to measure the masses of positive and negative τ's separately and therefore test the CPT theorem. A test performed by OPAL [37] gives the current lower limit, $(M_{\tau^+} - M_{\tau^-})/M_{Avg} < 3.0 \times 10^{-3}$ at 90% CL.

The current high statistic accumulated by the B-Factory experiments will allow a measurement with the same level of accuracy. In particular,

the Belle Collaboration has recently published a result on the measurement of the mass of the τ lepton and an upper limit on the mass difference between τ^+ and τ^- [38]. In this analysis, the τ mass is determined from hadronic decays of the τ, using the pseudo-mass technique descibed in [33] and in the previous section. The estimator of the τ mass is defined by: $M_{min} = \sqrt{2(E_{beam} - E_X)(E_X - p_X) + M_X^2}$. In absence of initial and final state radiation and assuming a perfect measurement of the four momentum of the hadronic system X, M_{min} is distributed below the τ mass and has an edge at M_τ. Intial and final state radiation and the finite momentum resolution of the detector smear the edge of M_{min} around M_τ. The threshold position obtained from the fit to the experimental M_{min} distribution is used as an estimator of M_τ.

The analysis is based on 253 fb^{-1} of data collected with the Belle detector. The data used are those on the Υ(4s) resonance, since the absolute beam energy calibration is better known for this sample than for the off-resonance data taken 60 MeV below the Υ(4s). $\tau^+\tau^-$ events are selected with one τ decaying leptonically ($l\bar{\nu}_l\nu_\tau$) and the other τ decaying into $3\pi^\pm\nu_\tau$ or $3\pi^\pm\pi^0\nu_\tau$. A set of preselection cuts on the total visible energy and the number of charged tracks in the selected $\tau^+\tau^-$ events are applied in order to remove BhaBha, $\mu^+\mu^-$ and two-photon background events. Particle identification is then applied in order to select events with one well identified muon or electron, recoiling against three charged pions. In case of the $3\pi^\pm\pi^0\nu_\tau$ decay mode, events with exactly one well identified π^0 are retained. The M_{min} distribution of the selected data events is fitted with the function:

$$F(x) = (p_3 + p_4 * x) \times \arctan((x - p_1)/p_2) + p_5 + p_6 * x \ . \qquad (6)$$

In case of the $\tau^\pm \to 3\pi^\pm\nu_\tau$ decay mode, the M_{min} data distribution is shown in Figure 6. The value of the parameter p_1 obtained from the fit is $p_1 = 1777.41 \pm 0.25$ MeV.

The difference between the threshold position obtained using Equation 6 and the true value of the M_τ obtained from MC is $\delta p_1 = 0.70 \pm 0.40$ MeV, where the uncertainty is dominated by the limited MC stastistic and the systematic of the fit procedure. The estimator value p_1 is corrected by δp_1 and the error on δp_1 is used as an estimate of the relative systematic uncertainty. Other systematic uncertainties are considered: calibration of the tracking system, choice of the fit range and shape of the threshold function, beam energy. The total systematic error is 0.62 MeV, giving a final result of $M_\tau = 1776.71 \pm 0.25(\text{stat}) \pm 0.62(\text{syst})$ MeV, in agreement with the PDG average [11]. The value of the τ mass estimator in the $\tau^\pm \to 3\pi^\pm\pi^0\nu_\tau$ decay mode is consistent within errors with the result from the $\tau^\pm \to 3\pi^\pm\nu_\tau$ decay mode.

The pseudo-mass method allows a separate measurement of the masses of the positively and negatively charged τ leptons. The M_{min} distributions

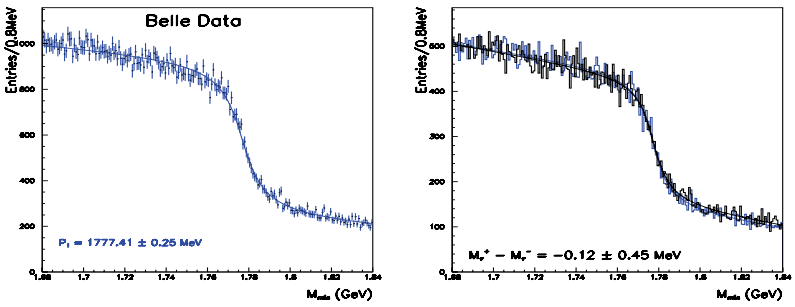


Figure 6: *τ mass analysis: (left) pseudo-mass distribution (M_{min}) for events selected in the $\tau^{\pm} \to 3\pi^{\pm}\nu_{\tau}$ decay mode. The point with error bars are data and the solid line is the result of the fit with the function in Equation 6. (right) pseudo-mass distribution (M_{min}) for τ^+ and τ^- decays in the $3\pi^{\pm}\nu_{\tau}$ decay channel. The solid lines are the results of the fit using the function in Equation 6.*

for τ^+ and τ^- decaying to $3\pi^{\pm}\nu_{\tau}$ are shown in Figure 6, together with the result of the fit. There is good agreement between the two distributions and the mass difference obtained from the independent fits to these distributions is $M_{\tau^+} - M_{\tau^-} = -0.12 \pm 0.45$ MeV. Most of the sources of systematic errors affect the result on τ^+ and τ^- in the same way, so that their contributions to the mass difference cancel. However, a mass shift can arise from the fact that particles and anti-particles interact differently with the detector material. The systematic uncertainty on the τ mass difference due to a possible shift in the measurement of the momenta of particles and anti-particles is estimated using data control samples and is found to be 0.15 MeV. An upper limit on the relative mass difference that includes both statistic and systematic errors is obtained using the frquentist approach described in [6]:

$$|M_{\tau^+} - M_{\tau^-}|/M_{Avg} < 5.0 \times 10^{-4} \text{ at } 90\% \text{ CL.} \quad (7)$$

The good agreement of the M_{min} distributions for positive and negative $\tau^{\pm} \to 3\pi^{\pm}\nu_{\tau}$ decays shows that, at the present level of experimental accuracy, CPT inveriance is respected.

5 Summary

The successful operation of PEPII and KEKB and the excellent performances of the *BABAR* and Belle detectors have allowed to obtain many interesting results in both charm and tau physics at the B-Factories.

The measurement of $D^0\overline{D}^0$ mixing in the $D^0 \to K^+\pi^-$ decay mode from the Belle experiment provides the world's most stringent limit on the mixing parameters x'^2 and y', assuming negligible CP violation: $x'^2 < 0.72 \times 10^{-3}$, $-9.9 \times 10^{-3} < y' < 6.8 \times 10^{-3}$ at 95% CL.

BABAR has measured the pseudoscalar decay constant f_{D_s} using charm-tagged $D_s^+ \to \mu^+\nu_\mu$ events and has obtained the most precise measurement to date of the ratio $\Gamma(D_s^+ \to \mu^+\nu_\mu)/\Gamma(D_s^+ \to \phi\pi^+)$. The measurement of the decay constant is $f_{D_s} = (279 \pm 17 \pm 6 \pm 19)$ MeV, in agreement with Lattice QCD predictions.

In both *BABAR* and Belle there have been several results from analyses looking for Lepton Flavour Violation in τ decay and production.

A recent result from Belle on lepton flavour violating decays $\tau^- \to l^- K_s^0$ has yielded the most stringent upper limit on the branching fractions of $\mathcal{B}(\tau^- \to e^- K_s^0) < 5.6 \times 10^{-8}$ and $\mathcal{B}(\tau^- \to \mu^- K_s^0) < 4.9 \times 10^{-8}$ at the 90% CL.

BABAR has presented for the first time at this conference a preliminary result on the search for the LFV processes $e^+e^- \to \mu^+\tau^-$ and $e^+e^- \to e^+\tau^-$. No evidence for signal is found and the 95% CL upper limits on the cross-sections is set at $\sigma_{\mu\tau} < 4.6\ fb$ and $\sigma_{e\tau} < 10.1\ fb$. The ratio of the cross-sections with respoect to the di-muon cross-section are measured to be $\sigma_{\mu\tau/\mu\mu} < 4.0 \times 10^{-6}$ and $\sigma_{e\tau/\mu\mu} < 8.9 \times 10^{-6}$. These are the first limits obtained at the energies accessible by the B-Factory detectors.

With the current high statistic of τ-pair events collected at the B-Factories it is possible to search for high multiplicity decays of the τ lepton, that can lead, if observed, to a more stringent limit on the tau neutrino mass. *BABAR* has recenlty published the world's most stringent upper limit on the $\tau^- \to 3\pi^-2\pi^+2\pi^0\nu_\tau$ decay: $\mathcal{B}(\tau^- \to 3\pi^-2\pi^+2\pi^0\nu_\tau) < 3.4 \times 10^{-6}$ at the 90% CL. This is more than a factor 30 improvement over the previously established limit. In addition, *BABAR* has obtained the first upper limit for the $\tau^- \to 2\omega\pi^-\nu_\tau$ decay mode: $\mathcal{B}(\tau^- \to 2\omega\pi^-\nu_\tau) < 5.4 \times 10^{-7}$ at 90% CL.

High precision measurements of the mass of the τ lepton can be performed at the B-Factories and the results can be used to test lepton universality. The Belle experiment has measured the mass of the τ lepton in the decay modes $\tau \to 3\pi\nu_\tau$ and $\tau \to 3\pi\pi^0\nu_\tau$. The preliminary result is $M_\tau = 1776.71 \pm 0.25(\text{stat}) \pm 0.62(\text{syst})$ MeV. The preliminary value of the upper limit on the relative mass difference between positive and negative τ leptons is $|M_{\tau^+} - M_{\tau^-}|/M_{Avg} < 5.0 \times 10^{-4}$ at 90% CL. At the present level of experimental accuracy, no violation of the CPT theorem is observed.

6 Acknowledgements

I would like to thank the Charm, Tau and Lepton working groups from *BABAR* and Belle Collaborations for their assistance and support in the preparation of

this talk.

References

1. *BABAR* Collaboration, B. Aubert *et al*, Nucl. Inst. Meth. A **479**, 1 (2002).
2. Belle Collaboration, A. Abashian *et al*, Nucl. Inst. Meth. A **479**, 117 (2002).
3. S. Kurokawa and E. Kikutani, Nucl. Inst. Meth. A **499**, 1 (2003).
4. G. Burdman and I. Shipsey, Ann. Rev. Nucl. Part. Sci. **53**, 431 (2003).
5. Belle Collaboration, L.M. Zhang *et al*, Phys. Rev. Lett. **96**, 151801 (2006).
6. G. Feldman and R.D. Cousins, Phys. Rev. D **57**, 3873 (1998).
7. C. Aubin *et al*, Phys. Rev. Lett. **95**, 122002 (2005).
8. CLEO Collaboration, M. Artuso *et al*, Phys. Rev. Lett. **95**, 251801 (2005).
9. CLEO Collaboration, M. Chadha *et al*, Phys. Rev. D **58**, 032002 (1998).
10. J. Stelzer, Ph.D. thesis, Stanford University (2006), SLAC-R-825.
11. Particle Data Group, S. Eidelman *et al*, Phys. Lett. B **592**, 1 (2004).
12. *BABAR* Collaboration, B. Aubert *et al*, Phys. Rev. D **71**, 091104 (2005).
13. Super-Kamiokande Collaboration, Y. Fukuda *et al*, Phys. Rev. Lett. **81**, 1562 (1998). SNO Collaboration, Q.R. Ahmad *et al*, Phys. Rev. Lett. **89**, 011301 (2002).
14. M.L. Brooks *et al*, Phys. Rev. Lett. **83**, 1521 (1999).
15. M. Ahmed *et al*, Phys. Rev. D **65**, 112002 (2002).
16. R. Barbieri, L.J. Hall, Phys. Lett. B **338**, 212 (1994).
17. J. Hisano *et al*, Phys. Lett. B **357**, 579 (1995).
18. R. Arnowitt, P. Nath, Phys. Rev. Lett. **66**, 2708 (1991).
19. *BABAR* Collaboration, B. Aubert *et al*, Phys. Rev. Lett. **96**, 041801 (2006).
    BABAR Collaboration, B. Aubert *et al*, Phys. Rev. Lett. **95**, 041802 (2005).
    BABAR Collaboration, B. Aubert *et al*, Phys. Rev. Lett. **92**, 121801 (2004).
    BABAR Collaboration, B. Aubert *et al*, Phys. Rev. Lett. **95**, 191801 (2005).

20. Belle Collaboration, K. Hayasasaka *et al*, Phys. Lett. B **613**, 20 (2005).
Belle Collaboration, K. Abe *et al*, Phys. Rev. Lett. **92**, 171802 (2004).
Belle Collaboration, Y. Yusa *et al*, Phys. Lett. B **598**, 103 (2004).
Belle Collaboration, Y. Yusa *et al*, hep-ex/0603036 (2006). Submitted to Phys. Lett. B.
Belle Collaboration, Y. Enari *et al*, Phys. Lett. B **622**, 218 (2005).
Belle Collaboration, Y. Miyazaki *et al*, Phys. Lett. B **632**, 51 (2006).

21. Belle Collaboration, Y. Miyazaki *et al*, hep-ex/0605025 (2006). Submitted to Phys. Lett. B.

22. J. Conrad *et al*, Phys. Rev. D **67**, 012002 (2003).

23. S. Jadach and Z. Was, Comput. Phys. Commun. **85**, 453 (1995).

24. S. Jadach, Z. Was, R. Decker and J.K. Kuhn, Comput. Phys. Commun. **76**, 361 (1993).

25. CLEO Collaboration, R.A. Briere *et al*, Phys. Rev. Lett. **90**, 181802 (2003).
OPAL Collaboration, R. Akers *et al*, Z. Phys. C **67**, 555 (1995).

26. B.F. Ward, S. Jadach and Z. Was, Nucl. Phys. Proc. Suppl. **116**, 73 (2003). E. Barberio and Z. Was, Comput. Phys. Commun. **79**, 291 (2004). D.J. Lange, Nucl. Inst. Meth. A **462**, 152 (2001). T. Sjöstrand, Comput. Phys. Commun. **82**, 74 (1994).

27. GEANT4 Collaboration, S. Agostinelli *et al*, Nucl. Inst. Meth. A **506**, 250 (2003).

28. T. Skwarnicki, Ph.D. thesis, Crakow Institute of Nuclear Physics (1986), DESY-F31-86-02.

29. K. Cranmer, Comput. Phys. Commun. **136**, 198 (2001).

30. *BABAR* Collaboration, B. Aubert *et al*, hep-ex/0604014 (2006). Accepted for pubblication in Phys. Rev. D.

31. S. Nussinov and M.V. Purohit, Phys. Rev. D **65**, 034018 (2002).

32. *BABAR* Collaboration, B. Aubert *et al*, Phys. Rev. D **72**, 012003 (2005).

33. ARGUS Collaboration, H. Albrecht *et al*, Phys. Lett. B **292**, 221 (1992).

34. R. Barlow, Comput. Phys. Commun. **149**, 97 (2002).

35. R.D. Cousins and V.L. Highland, Nucl. Inst. Meth. A **320**, 331 (1992).

36. BES Collaboration, J.Z. Bai *et al*, Phys. Rev. D **53**, 20 (1996).

37. OPAL Collaboration, G. Abbiendi *et al*, Phys. Lett. B **492**, 23 (2000).

38. Belle Collaboration, K. Abe *et al*, hep-ex/0511038 (2005).